AIDIC *Conference Series*, Vol. 10, 2011
Editor Sauro Pierucci
DOI: 10.3303/ACOS1110033
ISBN 978-88-95608-58-7 ISSN 2036-5969

DYNAMIC OF COUNTER-CURRENT HEAT EXCHANGERS AND A SIMPLE DISTILLATION COLUMN

Heinz A Preisig[a] and Jennifer Puschke[b]

[a] Chemical Engineering, NTNU, N – 7491 Trondheim, heinz.preisig@chemeng.ntnu.no
[b] RWTH Aachen, Templergraben 55, 52062 Aachen, Germany

In industry counter-current flow processes are common. Although these processes have been widely studied in literature, relatively little has been published on their dynamic characteristics. Two very common counter-current flow processes are heat exchangers and distillation columns. Ma's study (Ma, 1993) based on models of heat exchanger's dynamic behaviour reports and analyses the internal resonance effect, which is also earlier reported by Profos (1943) and others.
Here the study is extended to lumped models, which is a common approach taken. First for heat exchangers and thereafter for an extremely simplified distillation column. Not unexpectedly, the dynamic properties change gradually as the number of lumps increases towards the distributed systems. For high frequencies similar internal resonance effects evolve with the envelopes showing a very low-order behaviour, which though somewhat surprisingly is independent of the number of lumps. Finally we show that the eigenvalues of the normed system matrix lie on a circle in the complex plane for symmetrical plants.

1. INTRODUCTION

Many industrial processes are based on two phases exchanging material and/or energy. The two phases are passing each other either in co-current or counter-current fashion often arranged in stages in each of which one drives the system towards the equilibrium. The counter-current scheme is more commonly used, so we focus on this pattern. The body of literature on counter-current flow processes is very large, though if one focuses on the common dynamic characteristics of these processes, the number is rather small.
Heat exchangers are of particular interest. They are inherently distributed along the flow direction as well as in the direction of the conductive heat transfer. It is mainly the control community that has a strong interest in the dynamics of the process because the models are an ingredient into the controller synthesis. It is the first-order-plus-dead-time model that is most commonly used in this community, though, usually without a justification or analysis.
The history reflects that people have apparently been more interested in the subject in earlier days. One of the earliest work was done by Profos who analysed the dynamics of heat exchangers in his PhD thesis (Profos, 1943) using the frequency domain approach, where he also reports on the internal resonance effect. Stermole and Larson (1964) also present the frequency analysis and report experimental results, making reference to one of the earlier works by (Mozley, 1956). Cohen and Johnson (1956) worked very much along the same lines making reference to DeBolt's (1954) work, which though is not any more accessible, but is reported to have explored the internal resonance effects. Fanning and Sliepcevich (1959) take the same approach but explore the behaviour of a jacketed stirred-tank reactor. Also Hoeld (1974) shows the transfer functions of the distributed system and studies its properties.
These early project reveal all major issues: distribution effects on one hand yielding dead time behaviour along the flows, and principle low-order behaviour in the cross-stream transfer functions. Also the internal resonance effect is being discussed and experimentally verified.
These distributed models for heat exchangers are of infinite order whilst seemingly showing a low-order principle behaviour. As a consequence one would have expected that engineers and researcher would seek low-

Please cite this article as: Preisig H.A. and Puschke J., (2011), Dynamic of counter-current heat exchangers and a simple distillation column, AIDIC Conference Series, 10, 295-304 DOI: 10.3303/ACOS1110033

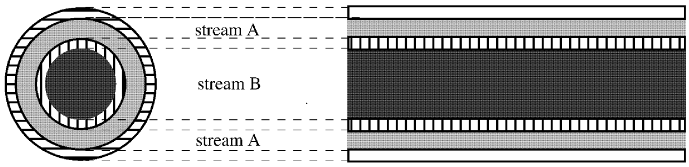

Fig. 1: Schematic Double-pipe heat exchanger

order approximations, which though took some time. One of the earlier ones picking up model reduction is Friedly (1972) who derived systematically reduced-order models from distributed models. This was further developed by Ma (1993) who derived a new set of high-fidelity low-order models also confirming the internal resonance effect, which years later again has been show to exist in an experimental study by Grimm (1999). Ma did her analysis and model reduction in the frequency domain, whilst Jogwar and Daoutidis (2009) and Heo et al. (2011) use singular perturbation to get a simplified model.

Besides the first-order-plus-dead-time models being used for control, approximate distributed models are most popular. They are derived by approximating the flow/heat-transfer system as a series of lumped systems, which, for a single-concentric-two-tube heat exchanger can be visualised as a set of slices, where each slice is seen as a modelling unit consisting of two ideally-stirred capacities linked through the conductive heat transfer through the fluid-separating wall. These models have the advantage that they are simple to explain, but have the disadvantage that they require a large number of lumps to get a good approximation of all the effects. Ma suggested at least 50 lumps to capture both the distribution effect and have a reasonable steady-state match without adding a correction factor. The models have though one main feature: to some extent they do model axial mixing and thus may describe the process better than a one-dimensional distributed description. The interest in these models is periodically showing in the literature. Most of the older references will make a mentioning, and also the control and design community has continuous interest (Mathisen et al., 1994) (Hawn, 2009) and very recently (Varbanov et al., 2011).

1.1 Ma's reduced-order models

In Ma's a distributed model for heat exchangers the temperatures on the inner and the outer tube are considered as continuous functions of time and spatial coordinates yielding a set of partial differential equations.

$$\text{Stream A:} \quad \frac{\partial T_A}{\partial t} + v_A \frac{\partial T_A}{\partial x} = d_A\,(T_B - T_A) \qquad , \quad d_a \quad := \frac{UA_{total}}{m_A c_{pA}}$$
$$\text{Stream B:} \quad \frac{\partial T_B}{\partial t} - v_B \frac{\partial T_B}{\partial x} = d_B\,(T_A - T_B) \qquad , \quad d_a \quad := \frac{UA_{total}}{m_B c_{pB}}$$

This model shows the presence of the internal resonance effect in the high frequencies domain.

$$\frac{dT_A(s)}{dx} + H_1 T_A(s) = H_2 T_B(s) \quad , \qquad H_1 = \frac{d_A + s}{v_A} \quad , \qquad H_2 = \frac{d_A}{v_A}$$
$$\frac{dT_B(s)}{dx} + H_3 T_B(s) = H_4 T_A(s) \quad , \qquad H_3 = \frac{d_B + s}{v_B} \quad , \qquad H_4 = \frac{d_B}{v_B}$$

With v :: stream velocity, U:: overall heat transfer coefficient, m:: mass hold up, c_p:: heat capacity, s :: Laplace variable. Which yields the four transfer functions

$$G_{11} := \frac{T_A(s)|_{exit}}{T_A(s)|_{inlet}} = \frac{(\lambda_1 - \lambda_2)e^{\lambda_2 L}}{(\lambda_1 + H_1) - (\lambda_2 - H_1)e^{(\lambda_2 - \lambda_1)L}} \quad G_{22} := \frac{T_B(s)|_{exit}}{T_B(s)|_{inlet}} = \frac{(\lambda_1 - \lambda_2)e^{-\lambda_1 L}}{(\lambda_1 + H_1) - (\lambda_2 - H_1)e^{(\lambda_2 - \lambda_1)L}}$$
$$G_{12} := \frac{T_A(s)|_{exit}}{T_B(s)|_{inlet}} = \frac{H_2[1 - e^{(\lambda_2 - \lambda_1)L}]}{(\lambda_1 + H_1) - (\lambda_2 - H_1)e^{(\lambda_2 - \lambda_1)L}} \quad G_{21} := \frac{T_B(s)|_{exit}}{T_A(s)|_{inlet}} = \frac{-H_4[1 - e^{(\lambda_2 - \lambda_1)L}]}{(\lambda_1 + H_1) - (\lambda_2 - H_1)e^{(\lambda_2 - \lambda_1)L}}$$

Ma successfully split the transfer function into a purely resonant part and a non resonance part. The non-resonance part describes the input/output behaviour of the cross transfer functions as a low-order transfer function, which when ignoring the wall dynamics is of first order. With wall capacity, a second-order behaviour provides an excellent approximation to a very high frequency, certainly above the practical applicable domain. These models are of high-fidelity, are analytical, low-order models and can match either the upper or the lower envelope of the distributed system or anything in between for that purpose. This is essentially the result of an asymptotic analysis mixed with a singular perturbation in the high frequency domain. The steady-state gain is extracted from the low-frequency part. The interested reader is referred to Ma's PhD thesis.

2. LUMPED MODEL OF THE HEAT EXCHANGER

A popular approach to modelling the double pipe heat exchanger is the "slicing" approach in which the heat exchanger is seen as a series of heat-exchanging, paired lumps. We follow Ma's work, who discusses several different cases that are based on different sets of assumptions. We focus on Ma's case I, where the assumptions are:

1. The total hold up of stream A is equal to the hold-up of stream B. Thus $m_A = m_B$ and with constant and both the same density is also $V_A = V_B$.
2. All lumps are of equal size in both streams.
3. Correspondingly: the heat transfer area to each pair of lumps is constant and equal: $A_i := A/n$, with A :: the total heat exchange area between stream A and stream B.
4. Heat is only transferred between two lumps with the same index, thus no axial heat transfer.

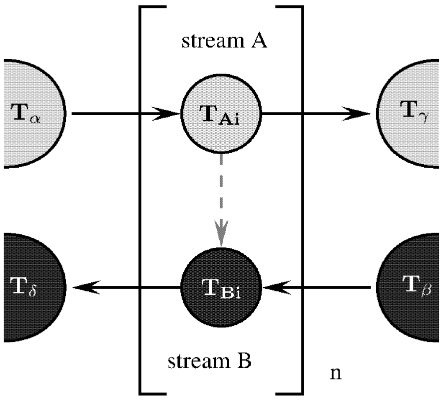

Fig. 2: Double-pipe heat exchanger as a series of slices each slice represented by two heat-connected lumps. The flow of A goes from α to γ and stream B β from to δ

2.1 State Space Model Equations for n Stages

The model of the sliced heat exchanger consists of a set of trivial mass balances and a set of energy balances, latter, for constant pressure, reducing to enthalpy balances. The balances in the state space spanned by the enthalpies in the individual nodes is readily transformed into the state space spanned by the lumps' temperatures if we assume constant properties. The resulting model is linear in the temperatures, and denoting the state vector by $x := (T_{a1} \ldots T_{an}, T_{b_1} \ldots T_{bn})^T$, the input by $u := (T_\alpha, T_\beta)^T$ and the output as $y := (T_\gamma, T_\delta)^T$ a straight linear-time-invariant system is obtained: $\dot{x} = Ax + Bu$ with the two matrices A and B being

$$A := \begin{pmatrix} -\tau_A - d_A & \tau_A & & & d_A & & & \\ & \ddots & \ddots & & & \ddots & & \\ & & \ddots & \tau_A & & & \ddots & \\ & & & -\tau_A - d_A & & & & d_A \\ d_B & & & & -\tau_B - d_B & & & \\ & \ddots & & & \tau_B & \ddots & & \\ & & \ddots & & & \ddots & \ddots & \\ & & & d_B & & & \tau_B & -\tau_B - d_B \end{pmatrix} ;\; B := \begin{pmatrix} 0 & 0 \\ \vdots & \vdots \\ \tau_A & 0 \\ 0 & \tau_B \\ \vdots & \vdots \\ 0 & 0 \end{pmatrix}$$

And the $y := Cx$ with the matrix $C := \begin{pmatrix} 1 & \cdots & 0 \\ 0 & \cdots & 1 \end{pmatrix}$ with $\tau_m := \frac{\dot{V}^m}{V/n}$; $d_m := \frac{k_m A_i}{\rho_m c_{pm} V}$, $m \in \{A, B\}$.

The quantities are: k_m :: heat transfer coefficient of stream m, A_i :: heat transfer area between two lumps, ρ_m :: density of the stream m, $\mathbf{c}_{pm}$ :: specific heat of stream m, V/n :: individual lump volume.

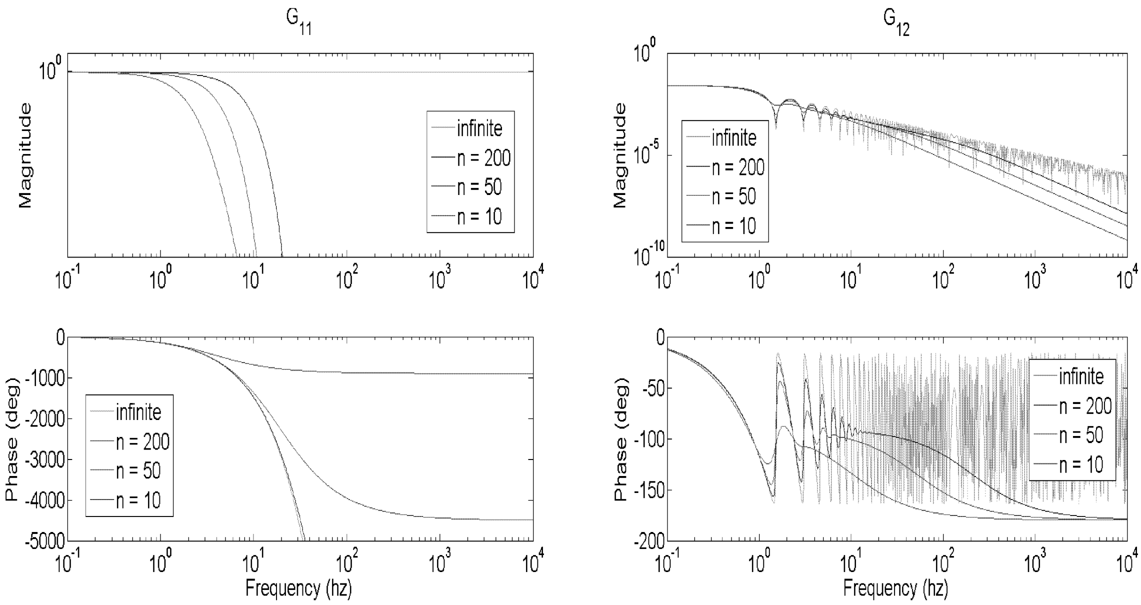

Fig. 3: Bode plots of the down stream transfer function G_{11} (left) and of the cross stream transfer function G_{12} (right) with different numbers of stages n. The parameters are chosen to be $d_A=d_B=0.01$; $\tau_A=1$; $\tau_B=1$.

2.2 Bode Plots

The dynamic behaviour of the models is depicted in Bode plots of the model's transfer functions. The transfer functions are derived by transforming the state space model into the frequency domain solving for the output $y = x$ in dependence of u. The transfer function matrix is then simply:

$$G=C(sI-A)^{-1}B$$

The down-stream transfer functions of input α to the output γ are similar to the one from the input β to the output δ and the same applies for the two cross-stream transfer functions. So we show only one of each, namely G_{11} for the down-stream transfer functions and G_{12} for the cross-stream transfer functions. As reference we show also the corresponding transfer functions of the distributed system, which corresponds to the distributed case.

Down Stream Response G_{11}: The behaviour of the transfer functions varies with the number of stages n. In the amplitude plot with an increasing number of stages n the slope of the amplitude decreases. As the number of stages approaches infinity the slope approaches zero. The latter implies that there exists only one gain. In the phase plot an increasing number of lumps increase the negative phase shift. For an infinite number of stages the phase lags go to minus infinity, which indicates the existence of a dead time. But there is not a resonance effect in the amplitude or the phase.

Cross Stream Response G_{12}: The Bode plot shows the resonance effect in amplitude and phase. Furthermore one observes that the curves show a first corner at the frequency of ω=1Hz for the chosen set of parameters. Above this corner frequency the slope in the amplitude plot of the resonance part is in average minus one. And in the phase plot the resonance part average is -90 degree. The transfer functions with the number of stages being small than infinite show a decaying resonance part with increasing frequency, which finally disappears. The apparent length of the resonance part depends on the number of stages: With an increasing number of stages, the resonance part grows longer until the infinite case, where the resonance part does not decay any more. Also the models with the number of stages being less than infinity, the final slope in the amplitude plot is -2 and the final phase lag is -180 degree. Hence this transfer functions show a second corner frequency under which the resonance part decays. Both corner frequencies depend on the number of stages.

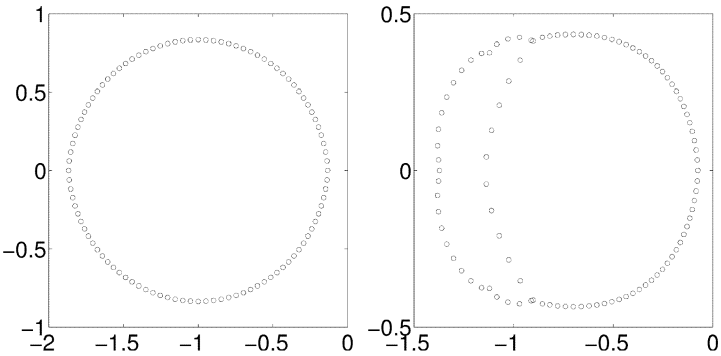

Figure 4: Normed eigenvalues of the system matrix in the complex plant for the lumped heat exchanger with 50 lumps. On the left is the case of equal hold-ups and on the right the hold up ratio is 1:2.5

2.3 Detailed Analysis of the Cross Stream Response

To get more information about the second-order behaviour of the cross stream response, one needs the pole excess of the transfer function. Due to the structure of the matrices B and C only four entries of the matrix $(\mathrm{Is} - \mathrm{A})^{-1}$ are relevant for the transfer functions matrix and only two of these entries for the cross-stream transfer functions. The zeros of the transfer functions are the zeros of the adjoint matrix $\mathrm{adj}(I\,s - A)$. For the number of stages n = *3 or 4* it is easy to show that the respective adjoint matrices have $2n$-2 zeros. Since the

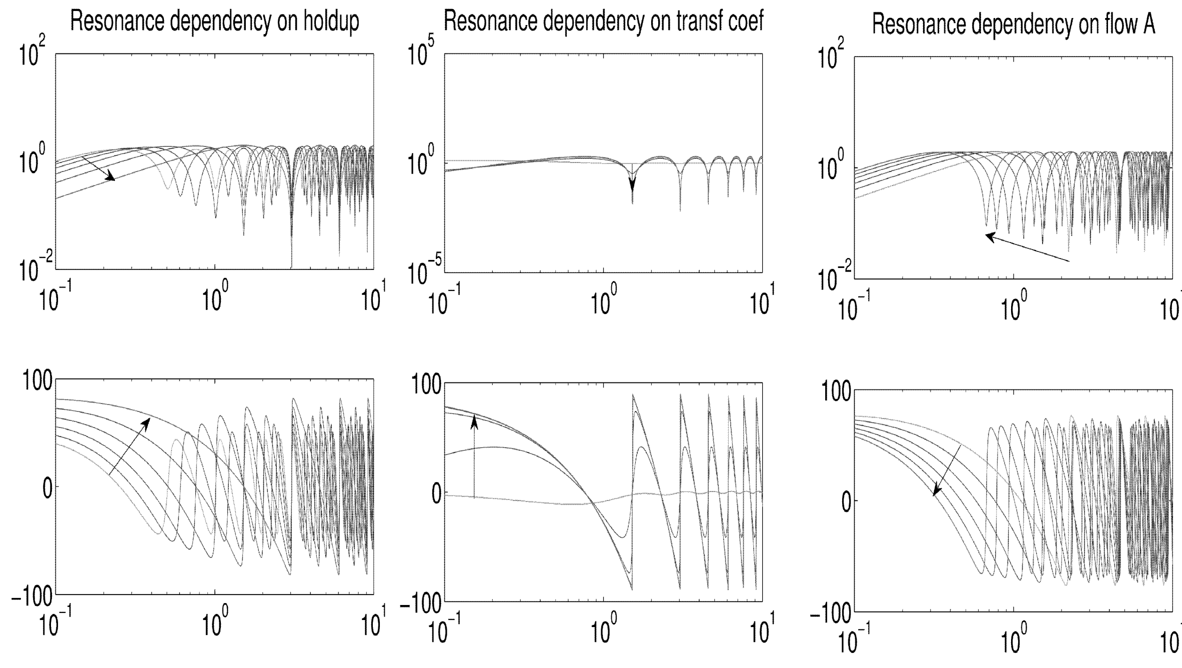

Fig. 5: Sensitivity of the resonance part to changes in the (left) total hold-up, which corresponds to changing the length at constant cross sections, (middle) transfer coefficient and (right) flow rate A. The arrows indicate decreasing values of the respective quantities.

poles are the eigenvalues of A, their number is $2n$. So the pole excess is 2n-(2n-2)=2, which explains the observed second-order behaviour. In addition, by closer examination of the poles, one finds that, for the given conditions, the normed eigenvalues of the matrix A form a circle with radius one and the centre at (-1,0) as shown in Figure 4. The shape changes with the relative sizing of the two streams. The circular feature does though not disappear, but in some cases two rings are formed, which when increasing the number of lumps join together. To form two rings the differences in the two stream dynamics must be significant. In Figure 4 the situation is shown where the split into two rings is just starting to emerge.

2.4 Parametric Sensitivity

The behaviour of the lumped model is certainly a function of the conditions applied to the plant and parameters characterising it. All characterising quantities are a function of the parameters: the gain, the corner frequencies of the approximate models as well as the resonance. The former two have been reported in Ma's thesis.
Figure 5 shows the effect on three of the main quantities on the resonance effect. Whilst one would expect that the resonance effect is of no practical relevance, literature indicates the existence of control problems that are due to the resonance effect Romero et al. (2005) .

2.5 A physical explanation of the resonance behaviours

The resonance behaviour is one of the striking characteristics of heat exchangers. Whilst it has been discovered by analysing models and later also experimentally verified in various instances, the phenomenon is not widely known. In fact it seems that it has never been really recognised in the sense of being text-book material. Reason is that the behaviour shows only at relatively high frequencies, though since it is also a function of the conditions and system properties, this may not always be the case.
The behaviour itself appears somewhat exotic at a first view, but looking at it in more detail reveals a very simple insight: If one injects a sinusoidal input signal on one side, it is apparent that through the transfer the wave is passed on to the other stream. For linear systems, the frequency of the two waves is identical, which to some extent also applies to non-linear systems. With the two streams moving with different relative speed to each other and the transfer being driven by the differences in the temperature in the two heat-communicating streams, the two extreme situations are when the two waves are in phase or if they are 90 degrees shifted at the exit point. In the first case, the temperature difference is minimal whilst in the second it is maximal.

3. LUMPED MODEL OF A SIMPLE DISTILLATION COLUMN

The heat exchanger discussed above is a counter current flow system, which is the source of the observed main characteristics of such processes. Distillations also are counter-current flow systems and as such should exhibit similar behaviours. From the analysis it became also apparent that these characteristics, whilst being a function of the process characteristic quantities and operating conditions, the qualitative features remain. This gave rise to attempt analysing distillations from the same point of view, which to the authors' knowledge has not been reported in the literature.

Here we repeat Ma's study with lumped models aiming at a comparison with distillation models. The model is constructed as a network of communicating capacities for each of which a mass and an energy balance is constructed. The energy balances are being transformed into the

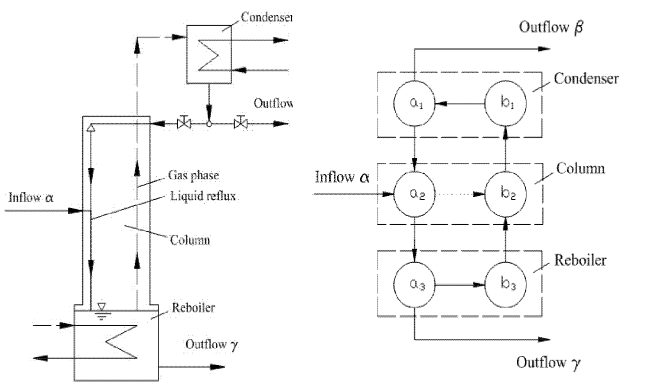

Fig. 6: Process of the distillation column (left) and the abstract model of the distillation column (right)

alternative state space of the temperatures all of which forms a set of ordinary differential equations. It is expected that, as the number of lumps approaches infinity, the solution approximates the solution of the distributed model hoping that the resonance effect shows also for low-order models. In a second step this is applied to a kind of a mass transport network representing a crude model of a distillation column.
Figure 6 depicts a distillation column and a minimal-stage abstraction there off which underlays also the construction of the model equations Dones and Preisig (2009) though with a large number of stages.

3.1 The State Space Model

The mass balances drawn for each lump. The key assumption making the analysis possible is to that the transfer between the two phases is a linear function of the effort variable. So we assume a linear transfer law making the mass transfer proportional to the composition. This approximates the ends of the column reasonably well, whilst if is not a good approximation for the middle part. The resulting balances combined with the linear transfer law are transformed from the state space spanned by the molar masses in each lump to the state space of molar composition for each lump. The total capacity of the plant is not considered in this analysis, thus the dynamics with regard to the composition is only modelled and analysed. The result is a standard linear-time-invariant state space model with the state x , input u and the output y being

$$x=\begin{pmatrix} c_{a1} & \cdots & c_{an} & c_{b1} & \cdots & c_{bn} \end{pmatrix}^T \; ; \quad u=c_\alpha \quad \text{and} \quad y=\begin{pmatrix} c_\beta & c_\gamma \end{pmatrix}^T \; .$$

The system matrices are:

$$A=\left(\begin{array}{cccccccccc}
-\tau_{a1}-\tau_\beta & & & & & \tau_{a1} & & & & \\
\tau_{a2} & -\tau_{a1}-d & & & & & d & & & \\
 & \ddots & \ddots & & & & & \ddots & & \\
 & & \tau_{an-1} & -\tau_{an-1}-d & & & & & d & \\
 & & & -\tau_{an} & -\tau_{an}-\tau_\gamma & & & & & 0 \\
0 & & & & & -\tau_{b1} & & & & \\
 & d & & & & & -\tau_{b2}-d & \tau_{b2} & & \\
 & & \ddots & & & & & \ddots & \ddots & \\
 & & & d & & & & & -\tau_{bn-1}-d & \tau_{bn-1} \\
 & & & & \tau_{bn} & & & & & -\tau_{bn}
\end{array}\right) ;$$

$$B=\begin{pmatrix} 0 & \cdots & 0 & \tau_\alpha & 0 & \cdots & \cdots & \cdots & 0 \end{pmatrix}^T \; ; \; C=\begin{pmatrix} 1 & 0 & \cdots & & & \cdots & 0 \\ 0 & \cdots & 0 & 1 & 0 & \cdots & 0 \end{pmatrix} ; \; D=\begin{pmatrix} 0 & 0 \end{pmatrix}^T$$

with $\tau_m=\frac{\hat{V}^m}{V}$ and $\tau_{i2}=\tau_{i3}\cdots=\tau_{in-1}$, $i\in\{a,b\}$

These sparse system matrices for the distillation column show a similar structure as the system matrices of the heat exchanger, with only a few elements being different.

3.2 Bode Plots

The transfer functions in the following Bode plots are obtained in the same way as this was done in the analysis of the heat exchanger (see Figure 7).
The curves in the magnitude plot of the cross transfer function from the input α to the output β in the Bode plots of Figure 7 shows again the resonance effect. This resonance part decays before the curves reach a multiple corner frequency, which depends on the number of stages *n*. With a larger number of lumps the resonance part reaches much further into the high frequency domain. If the number of stages goes to infinity one could assume, that there is only a steady state gain with resonance, whereas in the phase shift plot the resonance part does not appear at all. The general behaviour of the curves with the number of stages *n* going to infinity suggests the existence of a dead time.

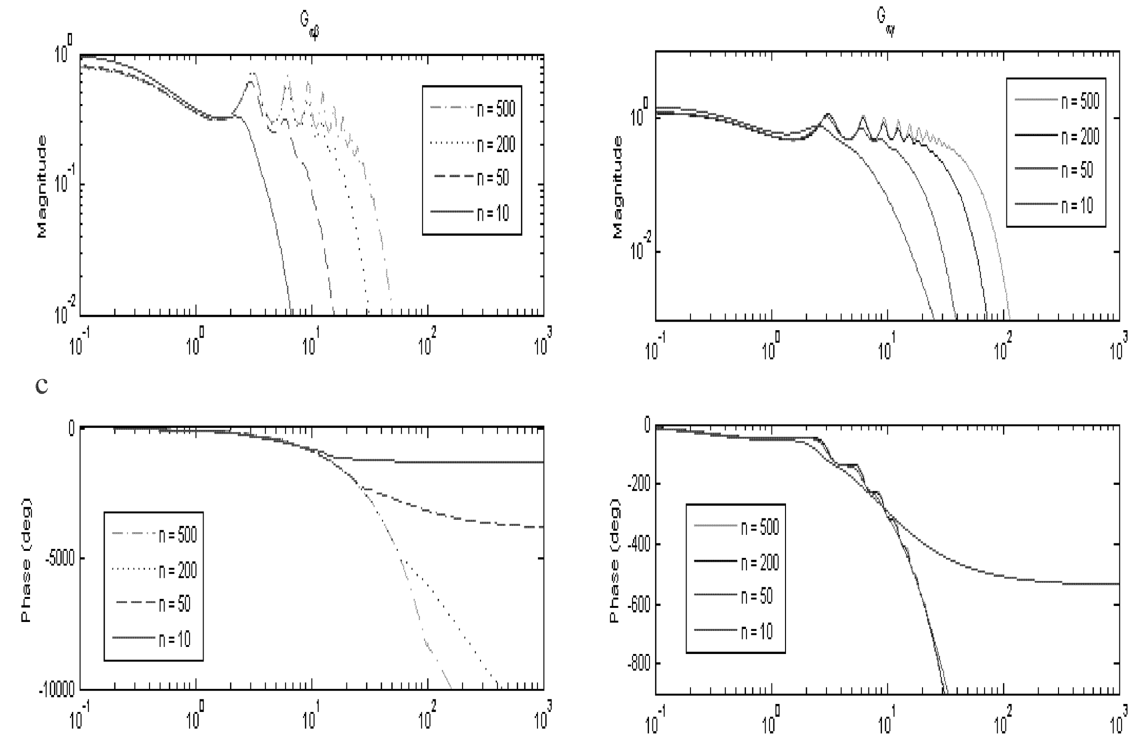

Fig. 7: Bode plots of the transfer function $G_{\alpha\beta}$ (left) from the input α to the output β and of the transfer function $G_{\alpha\gamma}$ (right) from the input α to the output γ with different numbers of stages n.

The magnitude plot of the transfer function from the input α to the output γ (see Figure 7) shows a comparable response behaviour as the transfer function from the input α to the output β. The differences are in the amplitude of the resonance part and the corner frequency. Also the phase plot of the of the transfer function from the input α to the output γ shows a resonant behaviour.

By closer examination of the poles in the complex plane, one finds again that the standardized eigenvalues of the system matrix A form a circle with radius one and the centred (-1,0), which is the same as for the lumped-model of the heat exchanger shown in Figure 3, both for symmetrical processes.

4. CONCLUSION

The *dynamic characteristics* of two counter-current processes are compared: a single tube heat exchanger and a staged linear distillation column. For both simple linear transfer models are assumed, which yield linear systems that are of very similar structure. The dynamic characteristics, which we visualise in Bode plots and eigenvalue plots, show that both systems exhibit similar behaviours, which is not a surprise.

One striking characteristic is the *internal resonance*. The physical explanation on how waves are being propagated in such systems gives a perfect logical explanation for the appearance of internal resonance effects: it is simply due to the phase shift between the two streams, which in turn are a function of the flow rates, the capacities and the transfer properties. In contrast to externally excited mechanical systems, the here-observed resonance effects are passive and do not result in a focus of the energy to the resonance frequency or the like.

The *eigenvalues* of the dynamic matrix, the ***A*** in the {A,B,C,D} representation of linear time-invariant systems, show regular patterns, which when normed with the number of nodes form a circle for symmetrical plants, meaning equal conditions on both sides. The circle approaches unity as the number of lumps increases with a shifted centre at -1 in the complex domain. The pattern also provides the insight that indeed there are a lot of

loops in such a system, which in turn is likely one of the sources for the oscillatory behaviour of production plants.
Both systems show *resonance effects* for some parts. Heat exchangers show it for cross-stream transfer functions, but not for down-stream transfer functions, whilst in distillation one finds the resonance also in the down stream transfer function, at least in the amplitude. In both cases, the magnitude of the resonance effect is a function of the number of lumps or stages.
In case of the heat exchanger the *pole excess* is 2, but the second corner frequency approaches infinity as the number of lumps approaches infinity. Thus for the distributed system the pole excess is only 1. This behaviour is also detected in the phase plot with a maximal phase shift of -180 degrees for finite number of lumps and -90 degrees for the distributed system.
The cross transfer functions for the distillation column behaves like a dead time for high frequencies, though the position of the multiple zeros shifts to higher and higher frequencies as the number of stages increases.

The analysis has been done on linear systems, with the obvious question rising on how this applies to non-linear processes, which the distillation is. Non-linear frequency analysis has a very sparse body of literature, but indications are that the frequency behaviour in its basic characteristics will not change significantly, but the main effect will be on the amplitude. Thus one can expect resonance behaviour in distillation, also when one considers the physical background of the phenomenon. Experimental verification should be attempted. Applications one can envision in the field of observing the internal conditions by adding small excitation signals to the input, enabling adaptive control, for example.

5. REFERENCES

Cohen W. C. and Johnson E. F. (1956) Dynamic characteristics of double-pipe heat exchangers. *Industrial and Engineering Chemistry* **48 (6)**, 1031-1034.

Dones I. and Preisig H. A. (2009) Graph theory and model simplification. Case study: distillation column. *ESCAPE 19* .

Fanning R. J. and Sliepcevich C. M. (1959) The dynamics of heat removal from a continuous agitated tank reactor. *AIChE J* **5 (2)**, 240-244.

Friedly J. C., (1972) *Dynamic Behaviour of Processes*. Prentice Hall, Englewood Cliffs, NJ.

Grimm R. (1999) Low-Order Modelling of the Dynamic Bahaviour of Heat Exchangers:Theory and Experimental Verification.

Hawn D. P. (2009) Development of a dynamic model of a counterflow compact heat exchanger for simulation of the gt-mhr recuperator using Matlab and Simulink.

Heo S., Jogwar S. S. and Daoutidis P. (2011) Dynamics and control of high duty counter-current heat exchangers. *19th Mediterranean Conference on Control and Automation; Corfu, Greece,June 20-23,* 1034-1039.

Hoeld A. (1974) Linear analytical one-dimensional model describing the frequency response behaviour of shell-and-tube type counterflow heat exchangers with respect to primary and secondary inlet temperature and mass flow perturbations. *Nuclear Engineering and Design* **26**, 231-241.

Jogwar S. S. and Daoutidis P. (2009) Multi-scale dynamics in counter-current heat exchangers. *17th Mediterranean Conference on Control and Automation* , 169-174.

Ma X. H. (1993) Dynamic Modelling, Simulation and Control of Heat Exchangers.

Mathisen K. W., Morari M. and Skogestad S. (1994) Dynamic models for heat exchangers and heat exchanger networks. *Comp & Chem Eng* **18**, S459-S463.

Mozley J. M. (1956) Predicting Dynamics of Concentric Pipe Heat Exchangers. *Ind Eng Chem* **48 (6)**, 1035-1041.

Profos P. (1943) Die Behandlung von Regelproblemen vermittels des Frequenzganges des Regelkreises.

Romero J. A., Campo A. and Albertos P. (2005) Control of heat exchanger using an iterative approach. *Proceedings of the 16th IFAC World Congress* **16 (1)** .
Stermole F. J. and Larson M. A. (1964) The dynamics of flow forced distributed parameter heat exchangers. *AIChE Journal* **10 (5)**, 688-694.
Varbanov P. S., Klemes J. J. and F F. (2011) Cell-based dynamic heat exchanger models--Direct determination of the cell number and size. *Comp & Chem Eng* **35**, 943-948.